Magnesium Technology 2013
Edited by: Norbert Hort, Suveen N. Mathaudhu, Neale R. Neelameggham, and Martyn Alderman
TMS (The Minerals, Metals & Materials Society), 2013

SYNTHESIS OF DISINTEGRABLE METAL COMPOSITE FOR OILFIELD APPLICATIONS

Zhihui Zhang, Bobby Salinas, Caleb Newman and Zhiyue Xu
Baker Hughes Incorporated; 14990 Yorktown Plaza Drive; Houston, TX, 77040, US

Keywords: Composite, Disintegrable, Corrosion, Hydraulic Fracturing

Abstract

Lightweight metal composites were traditionally developed for weight-critical applications. Recently, significant efforts have been made to improve the corrosion performance. In this study we report the synthesis of a novel type of high-strength metal composites with enhanced corrosion rate for use in self-disintegratable tools in oil and gas wells. The composites were fabricated through a powder metallurgy procedure by consolidating reactive metal powders that were coated with nanoscale metallic and/or ceramic coatings. The interaction between the metal matrix and coating was studied using X-ray diffraction, differential scanning calorimetry, and electron microscopy. The composites exhibit simultaneous high strength (up to 460 MPa) and two orders of magnitude increase in the corrosion rate (i.e., 250 mg/cm^2/hr) under saline water. The corrosion behavior and associated field applications are described.

Introduction

The need for lightweight metal composites has recently generated renewed interest, given their potential to improve energy efficiency and limit carbon dioxide emissions- particularly in light of recent combinations with nanotechnology, which may offer them unusual physical, mechanical and other functional properties. Many inquiries/investigations have been directed toward the development of magnesium composites reinforced with nanoparticulates such as SiC, Y_2O_3, Al_2O_3, and carbon nanocubes because of their intrinsic low density and superior mechanical properties (for purposes such as weight savings and/or better design of weight distribution and balance in the aerospace, automobile and sporting goods industries). In most of these applications, however, corrosion prevention and mitigation represents a challenge, limiting their wide-spread use. In addition, because of the biocompatibility of magnesium and its closeness of Young's modulus to that of the human bone, magnesium alloys have been considered a promising material for biodegradable implant application (to thwart the need to re-open an implant after healing). In this case, a controlled manner of corrosion is preferred. Controlled corrosion of certain structural components and parts also represents tremendous technical and economic advantages in oil and gas well completions. In recent decades, production of natural gas from entrapped low permeability shale formations (shale gas) has grown rapidly from virtually nothing in 2000 to more than 10 billion cubic feet per day in 2010. Shale gas supply is expected to continue increasing, and account for more than 50 percent of the total US natural gas production by the 2030s. To extract natural gas economically from the low permeability shale plays, the wellbore must be drilled horizontally and completed with multistage hydraulic fracturing along the shale formations (ranging from ten to hundreds of meters in thickness) to extend the production zone. One-trip deployments offer an efficient multistage fracturing system by using setting balls and ball seat design to activate one sleeve at a time, thus allowing the entire lateral to be fractured stage by stage in the horizontal wellbores. If the balls and ball seats must be removed mechanically from the well after fracturing to clear the pathway for production, this means re-entering the wellbores with costly tools and decreasing system efficiency. One solution utilizing the wellbore fluid to flow the setting balls back may alleviate the problem, but the density requirement for flowback leaves these lightweight materials, such as phenolic, weak and prone to severe plastic deformations. If the formation fluid pressure is very low, it can be difficult to get the frac balls off seat or to flow back to the surface. The balls can also be obstructed by the residual frac/formation sand when production velocity is not high enough. Therefore, the superior solution is to develop strong and reliable materials so they are able to perform their functions during fracturing, the tool then chemically disintegrates itself under the wellbore fluids after the fracturing is completed [1]. Although materials possessing individual high strength, light weight or high disintegration rates have been well documented, integrating these three functions into one material still represents a technical challenge. This paper presents a novel composite, disintegrable metal matrix composite (DMMC), to meet such demand. The base materials were selected with three criteria to meet the interventionless downhole application requirement: (1) light weight, (2) controllable disintegration rate when engineered with corrosion enhancer constituents, (3) achievable high strength by microstructural and/or process engineering. Light weight is necessary for the setting balls to flow with wellbore fluid during deployment. A controllable disintegration rate requires the DMMC material to not only exhibit a wide range of disintegration rates for different applications, but also corrode slowly before a critical service time (for the system to complete its function) and then disintegrate rapidly following the service. In general the setting ball should disintegrate enough to become unseated in hours. During deployment, the ball can travel with a flow speed as high as 160 km/hr. Therefore, the DMCC material must also exhibit high strength and toughness.

Experimental Procedures

Reactive metallic powders were coated with metallic and Al_2O_3 coatings with a thickness in the range of 30~1000 nm using chemical vapor deposition (CVD). Table 1 lists the materials and sample designations in this study. The coated powders were then consolidated using a powder hot forging process with a pressure of 400 to 600 MPa at a processing temperature between 250 and 550 °C.

The microstructure was characterized using X-ray diffraction (XRD), differential scanning calorimetry (DSC), scanning electron microscopy (SEM) and transmission electron microscopy (TEM). The XRD was conducted on a Scintag X1 diffractometer using CuKα radiation. The DSC was carried out using a TA Instruments Q10 differential scanning calorimeter. The SEM was conducted in a FEI Quanta 600 scanning electron microscope. The TEM was conducted in a JEOL JEM2100F transmission electron microscope.

The corrosion rate was evaluated by weight loss in a 3% KCl solution at 100 ℃, a modified corrosion immersion test method to simulate the downhole fluid environment. Cylinder test coupons were machined to a dimension of 12.7 mm in diameter and 25.4 mm in length. For each data point, the corrosion rate, or disintegration rate, was determined from the average of three coupons. Each sample coupon was measured prior to and after the test and the weight loss rate of corrosion/disintegration (disintegration rate, mg/cm^2/hr) was calculated with a time span of 24 hrs.

The mechanical properties were evaluated with compressive tests. Cylinder specimens were cut to a dimension 12.7-mm diameter and 25.4-mm length, according to ASTM E9 standard. The mechanical tests were conducted on a MTS electromechanical test machine with a load cell capacity of 100kN.

Table 1

Sample	Coating	
	Structure	Total thickness, nm
A	Base/M/Bond	1250
B	Base/M/Bond	1300
C	Base/M/Bond	1400
D	Base/Al_2O_3/Bond	2000

Results and Discussion

The DMMC matrix powder was produced via inert gas atomization with an average particle size of ~100 μm. Figure 1 shows a cross-section view of the DMMC powder following CVD coating (i.e. sample C). The powder particle was first coated with a metallic layer (designated as M hereafter) that has a standard electrode potential higher than Zn to form galvanic cell reactions when exposed to wellbore fluid. A bond coat was subsequently applied on top of the M layer to prevent contamination and facilitate consolidation. A series of different thicknesses were selected to study their effect on disintegration rates and mechanical strength (i.e. two key criteria for the ball deployment under the wellbore condition), as listed in Table 1. An Al_2O_3 layer substitute for the M layer was also selected for comparison purpose to differentiate the effect of M layer on the mechanical strength and disintegration rate. The chemical reactivity between the matrix and bond layer was accessed by using DSC scanning the CVD-coated powder with a heating rate of 10 °C/min, as shown in Figure 2. A moderate reaction between the bond coat and matrix powder is favored to form a metallurgical bond during the powder consolidation. The endothermic reaction at approximately 439 °C is expected from the phase diagram between the matrix alloy and bond coat. The sample with M layer shows a much lower reaction peak than the sample with Al_2O_3 layer. The DSC result is consistent with the microscopic examination showing that the M layer is almost fully continuous, whereas the Al_2O_3 layer is subjected to certain microporosity.

Despite different thickness and chemistry, the CVD coating was able to well bond to the matrix powder and undergo powder consolidation. As shown in Figure 3, the CVD coating formed a continuous network in the consolidated bulk composites, with no cracking or splitting observed between the matrix and M layer (Figure 3a) or Al_2O_3 layer (Figure 3b).

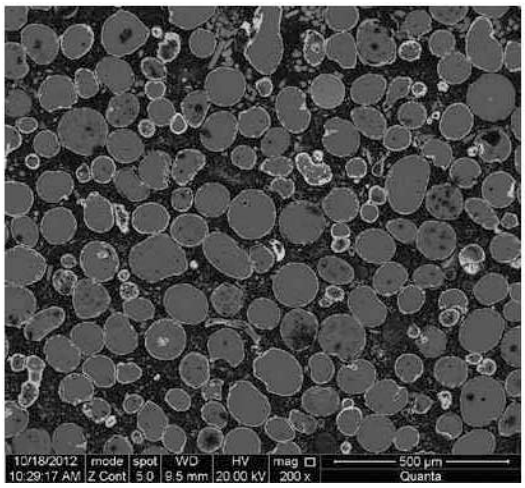

Figure 1. CVD coated DMMC powder.

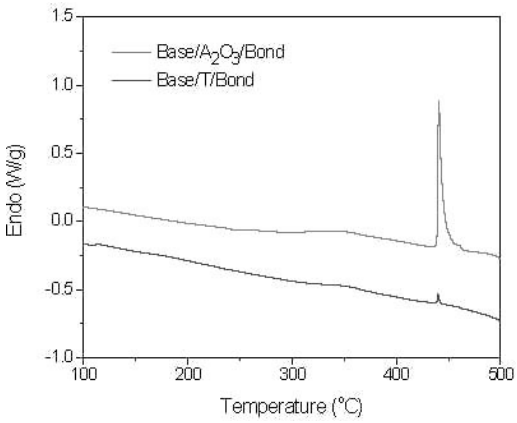

Figure 2. DSC continous heating curves of DMMC powders at a heating rate of 10 °C/min.

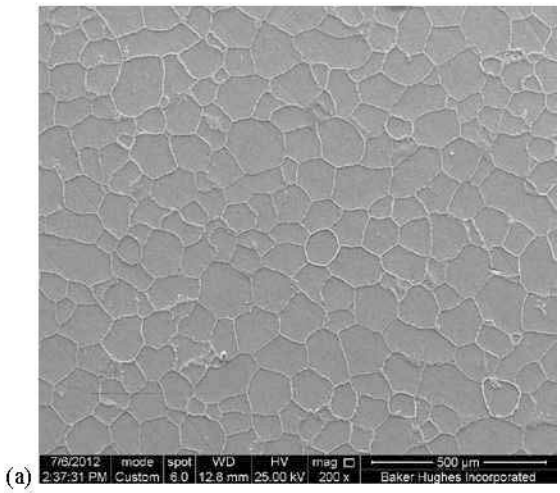

(a)

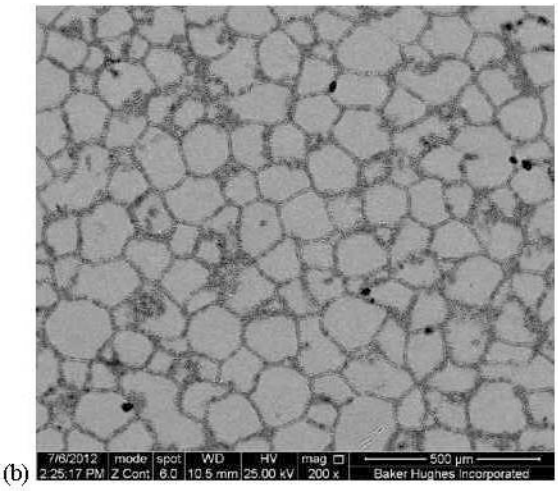

(b)

Figure 3. SEM micrographs of bulk DMMC composites: (a) Sample A, (b) Sample D.

Figure 4 shows a TEM bright field image taken from sample D. The interface between the matrix and CVD coatings (marked by a thick arrow) remained intact without interfacial debonding or delamination. Precipitates on the order of 200 nm were present in the matrix. XRD analysis (not shown here) indicated the majority of secondary phases were indexed to be $Mg_{17}Al_{12}$. The presence of $Mg_{17}Al_{12}$ was also identified in other samples by XRD.

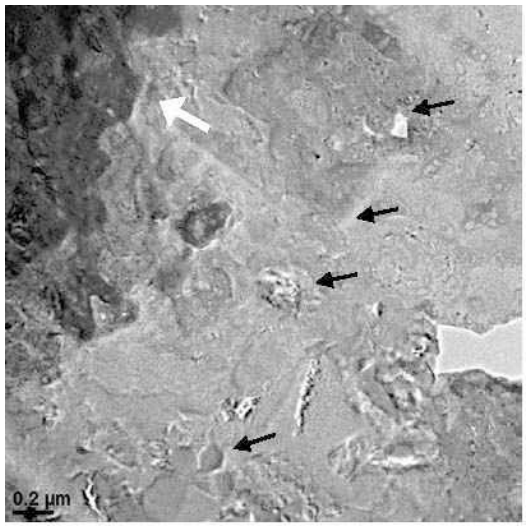

Figure 4. TEM bright field image from sample D.

The mechanical properties and rate of disintegration are shown in Figure 5(a) and (b), respectively. The disintegration rate for the first few hours (i.e. ~4 hours) are slightly lower and then become flat to nearly a constant up to 120 hours. An initial lower corrosion rate is an advantage to ensure the service functionality before the material is ready to dispose itself. In this study, the reported disintegration rate was measured with an average rate spanning 24 hrs. During application, a rate of 50 to 100 $mg/cm^2/hr$, or a diameter reduction rate up to 0.01 to 0.03 inch/hr is usually required to fit the hydraulic fracking operations where ball dismount time should match the shut-in time before production flows can be established. The dismounted ball could then be opted for either flowing back or disintegration by itself under the wellbore fluid, ensuring the elimination of any production pathway blockage. During the self-disposing application, the ultimate compressive strength is often cited as the criterion to determine the maximum pressure it can hold from the wellbore fluid. The compressive strength, as well as the strain to failure obtained from the DMMC composites is shown in Figure 5(a). The strain to failure is dependent on the chemistry of the coating and other factors such as processing defects; as a result, the compressive strength did not show a clear trend when compared to the coating thickness. This suggests an analysis at fixed plastic strain. Considering that moderate plastic deformation is required in the actual application, we selected an offset strain of 2% in this study to understand the strengthening mechanisms operating in the network DMMC (which was also plotted in Figure 5(b). The strengthening contributions in the DMMC were examined in order of (1) solid solution strengthening, (2) grain boundary strengthening, (3) Orowan strengthening, (4) internal stress strengthening, and (5) work hardening.

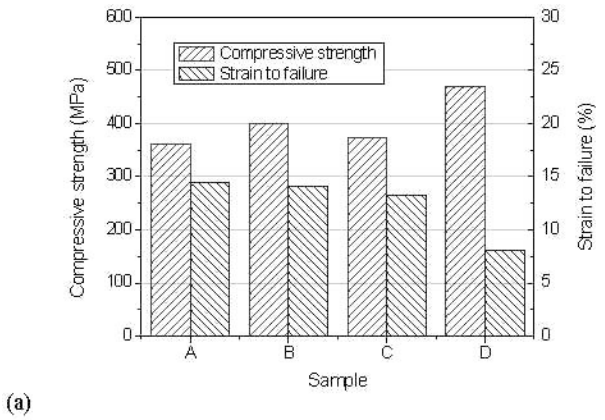

(a)

(b)

Figure 5. (a) Compressive strength and strain to failure of DMMC composites, (b) 2% offset stress and disintegration rate as a function of coating thickness and chemistry.

In dilute Mg-Al alloys, the yield stress increment as a result of dissolving solute atoms can be written as [2]:

$$\sigma_{ss} = M \cdot B \cdot c^n \quad (1)$$

where M is the Taylor factor and is usually taken to be 4 to 6.5. The term c is the solute concentration and n = 1/2 ~ 2/3. The term B is the solid solution hardening rate can be determined experimentally. From ref.[2], B = 21.2 MPa (at.)$^{-1/2}$ and M = 5.6 with n = 1/2. Here, the solute concentration c was estimated with an EDX line scan, as shown in Figure 6.

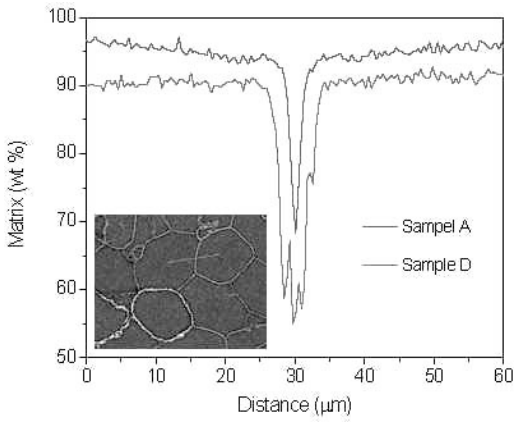

Figure 6. EDX line scan across the CVD coating

Grain boundary strengthening (or Hall-Petch strengthening) represents a strength advantage with a powder metallurgy processing technique over the conventional ingot metallurgy due to the rapid cooling process involved in the feedstock powder production. The yield stress as a function of grain size can be expressed as:

$$\sigma_{H-P} = \sigma_0 + k_y d^{-1/2} \quad (2)$$

where σ_0 = 11 MPa is the yield stress of coarse-grained counterpart, and k_y = 0.21 MPa $m^{1/2}$ is the Hall-Petch slope. The term d is the grain size and is determined to be ~40 to 50 μm by the line intersection method.

The Orowan strengthening results from the interaction of fine precipitates and dislocation in the matrix. The Orowan strengthening can be formulated as [3]:

$$\sigma_{OR} = M \frac{0.4Gb}{\pi(1-\nu)^{1/2}} \frac{In(\bar{d}_p / b)}{\bar{\lambda}_p} \quad (3)$$

where M is the Taylor factor (taken as 5.6), G is the shear modulus (17.4 GPa), b is the Burgers vector (0.32 nm), ν is the Poisson's ratio (0.29). $\overline{d_p}$ and $\overline{\lambda}_p$ are the average particle size and interparticle spacing. The value of $\overline{d_p}$ and $\overline{\lambda}_p$ was measured to be 200 nm and 500 nm, respectively, as shown in Figure 4.

The rate of work-hardening in these samples is dependent on factors such as solute atom concentration and material thermomechanical history; hence, it is generally difficult to formulate. Owing to the fact that all these samples underwent an identical processing procedure, only the effect of solute concentration is considered here using interpolation:

$$\sigma_{W-H} = \Delta\sigma(c_0) + \frac{\Delta\sigma(c_1) - \Delta\sigma(c_0)}{c_1 - c_0} \cdot (c - c_0) \quad (4)$$

where $\Delta\sigma(c_0)$ = 41.2 MPa and $\Delta\sigma(c_1)$ = 82.7. MPa are the work hardening rates for the pure metal and 10 wt% solid solution, respectively, which are determined experimentally from consolidated samples without the CVD coating.

Plastic deformation of a composite produces internal stress which impedes the flow by a stress proportional to the volume fraction of the inclusions and to the applied plastic strain. An estimate of the contribution from network phases was be made with the methods of Brown and Clarke [4]. The mean stress in the matrix due to inclusion is written as:

$$\sigma_{IS} = 4\gamma D G f \varepsilon_p \quad (5)$$

where γ = 1/2(1-ν) is an inclusion shape accommodation factor and ν the Poisson's ratio. $D = G^*/[G^* - \gamma(G^* - G)]$, where G and G^* are the shear modulus of the matrix and inclusion, respectively. The term D depends on the geometry of the inclusion and the ratio of the shear modulus of the inclusion and the shear modulus of the matrix. ε_p is the plastic strain and f is the volume fraction of the inclusion.

The predicted contributions to the flow stress (equations (1)-(5)) are summarized in Table 2. The total flow stress was calculated assuming simple additivity of each individual component. Table 2 indicates an agreement between the predictions and the experimental measurements. The theoretical estimate is on the conservative side, especially for sample D (when the network becomes more rigid due to Al_2O_3). This discrepancy becomes exacerbated if the root mean square law is assumed for each individual contribution. It should bear in mind that the simplified mean stress approach (i.e. equation (5)) ignores the continuous networking effect, which is expected to affect the deformation mode. Nevertheless, the equation (5) shows the CVD coating can significantly influence the material deformation behavior in addition to the disintegration rate.

Table 2

Sample	σ_{SS}	σ_{H-P}	σ_{OR}	σ_{W-H}	σ_{IS}	Cal.	Exp.
A	25.2	58.8	52.3	59.9	10.3	210.7	213.6
B	24.6	59.9	50.7	60.8	25.7	224.8	227.4
C	24.0	61.0	51.6	62.0	51.4	252.1	261.8
D	35.8	63.5	54.2	82.7	132.9	368.6	413.4

In summary, lightweight DMMC composites were successfully engineered with high disintegration rates up to 400 mg/cm^2/hr, and compressive strengths up to 460 MPa. A combination of mechanical strength and high disintegration rates enable the DMMC material to be a candidate for many interventionless downhole applications. The strengthening contributions were examined to shed light on ways of achieving even higher strength (>700 MPa) with high disintegration rates for future DMMC material development.

Acknowledgment

This research was sponsored by Baker Hughes and accomplished under the Type-1 research program.

References

1. Z. Xu, G. Agrawal, and B.J. Salinas, "Smart Nanostructured Materials Deliver High Reliability Completion Tools for Gas Shale Fracturing" (Paper presented at the SPE Annual Technical Conference and Exhibition 2011, Denver, Colorado), SPE 146586
2. C. H. Cáceres and D.M. Rovera, "Solid solution strengthening in concentrated Mg-Al alloys", Journal of Light Metals, 1(3) (2001), 151-156.
3. B. Q. Han et al., "Mechanical properties of an ultrafine-grained Al-7.5 pct Mg alloy", Metallurgical and Materials Transactions A, 34(3) (2003), 603-613.
4. L. M. Brown and D.R. Clarke, "Work hardening due to internal stresses in composite materials", Acta Metallurgica, 23(7) (1975), 821-830.